

Inhibiting the Appearance of Green emission in Mixed Lead halide Perovskite Nanocrystals for Pure Red Emission

Mutibah Alanazi¹, Ashley R. Marshall^{1,2}, Yincheng Liu^{1,3}, Jinwoo Kim¹, Shaoni Kar^{1,2}, Henry J. Snaith¹, Robert A. Taylor¹, and Tristan Farrow^{*4,1}

¹Clarendon Laboratory, Department of Physics, University of Oxford, Parks Road, Oxford, OX1 3PU, U.K.

²Helio Display Materials Ltd., Wood Centre for Innovation, Oxford, OX3 8SB

³Institute of Materials Research and Engineering, Agency for Science, Technology and Research (A*STAR), 2 Fusionopolis Way, Singapore 138634, Singapore

⁴NEOM Education, Research and Innovation Foundation, and NEOM University, Tabuk 49643-9136, Saudi Arabia

*Corresponding authors: tristan.farrow@cantab.net

Experimental Methods

Synthesis

Nanocrystal Synthesis: PbX₂ powder (0.2 mmol), CsX powder (0.2 mmol), OA (0.5 mL), OAm (0.25 mL) and DMAI (for the A-site modified NCs) were added to 5 mL of dimethylacetamide (DMAc) and stirred to dissolve for 60 mins at room temperature. A portion (3 mL) of the obtained mixture was swiftly injected into 30 mL chlorobenzene or chloroform under vigorous stirring. After stirring, the resulting solution was mixed with methyl acetate in a 1:2 ratio (v/v) and centrifuged for 5 min at 7500 revolutions per minute (rpm). After centrifugation, the supernatant was discarded, and the precipitate was dispersed in hexane. Stable CsPbI₂Br NC ink (~10 mg mL⁻¹) was obtained by removing larger particles after centrifuging the crude dispersion for 5 min at 3000 rpm. Further washing (repetition of fast and slow centrifugation steps) can be done for device application.

Film Fabrication (solution processing): The ITO substrates underwent a cleaning process involving sequential sonication in DECON-90, DI water, acetone, and IPA for a duration of 15 minutes each. Following that, the substrates were subjected to UV-ozone treatment for a further 15 minutes. The films utilized for fundamental characterisation and devices were fabricated using the spin-coating technique on ITO/PEDOT:PSS substrates. The PEDOT:PSS solution was subjected to a spin-coating process in ambient conditions, with a rotation speed of 5000 rpm for a duration of 40 seconds. Subsequently, the coated film was subjected to annealing at a temperature of 150 °C for a period of 12 minutes. Afterwards, the specimen was transferred to the glovebox antechamber and left to undergo a drying process for a duration of 20 minutes. Then, NC ink was spin-coated for 40 seconds at 1500 rpm in the glovebox. Any residual solvent was evaporated at 50 °C for a duration of 10 minutes.

Optical Characterization

Photoluminescence spectroscopy: The substrate was mounted in a Janis continuous-flow helium cryostat and the temperature was varied between 4.2 K and room temperature by a Lakeshore 331 temperature controller. Optical characterization was conducted using a confocal micro-photoluminescence set-up. The pump was a continuous wave wavelength laser source (405 nm) and a pulsed variable-wavelength laser source (NTK SuperK Extreme) operating at a maximum frequency of 78 MHz. A 100× magnification apochromatic objective was used in the confocal set-up to focus the pump beam to a spot size of ~1 μm² and to collect the luminescence. The spectra data of PL spectroscopy was collected using a SpectraPro HRS spectrometer.

Time Resolved Photoluminescence (TRPL) spectroscopy: TRPL measurements were carried out with a time-correlated single photon counting system (PicoHarp 300) coupled with 2 single photon avalanche diodes (MPD PDM) and the time constants were determined using EasyTau.

UV-Vis absorption : Separately, absorbance spectra were measured with a Varian Cary 300 Bio UV-Visible spectrophotometer with a 50×50 mm reflective neutral density filters with an optical density of 3.0 (made out of UV fused silica).

4.2.4 X-ray diffraction spectroscopy: XRD diffractograms were obtained using a Panalytical X'Pert Pro X-ray diffractometer with a Cu-alpha source ($\lambda = 1.54 \text{ \AA}$).

Transmission Electron Microscope (TEM): PNC solutions (~50 mg/mL) were diluted to about 10 mg/mL (as indicated by their optical densities measured on a UV-visible spectrometer) in 9:1 volume ratio of toluene: hexane solvent. This was then drop cast onto a carbon-coated copper TEM mesh-grid and the samples left to dry in the glovebox antechamber for about an hour. The TEM imaging was then done on a JEOL JEM-2100 microscope operating an LaB6 source and equipped with

an Oxford instrument 80 mm thin window EDS detector and a Gatan Orius CCD camera. The ImageJ software was using to analysis the crystal Size.

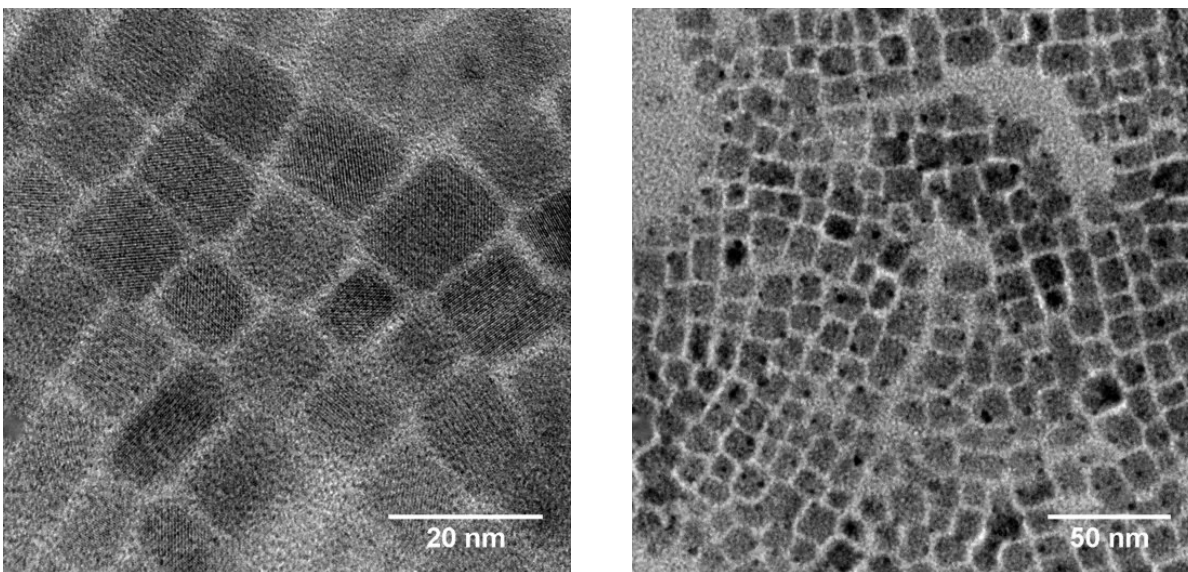


Figure S1. Transmission electron microscopy (TEM) images depicting nanocrystals composed of CsPbI₂Br.

The photo-oxidation mechanism of CsPbI₂Br nanocrystals and thin films.

The absence of a green glow in pristine thin films is due to the accumulation of Pb⁰ and I₃⁻ defects, which increase the lattice energy of pristine thin films, and then diffuse to grain boundaries, forming an I-rich phase due to the presence of multiple surface defects in the thin film compared to nanocrystals (e.g. dangling bonds and uncoordinated (Pb²⁺ ions). This can further refer to the fact that the diffusion of both Pb⁰ and I₃⁻ defects in thin films has a higher propensity to migrate from the bulk to the surfaces of grains and grain boundaries along a vertical pathway than pristine nanocrystals. The inter-diffusion rates for this migration range approximately between 10¹⁹ to 10²⁰ m²s⁻¹. In specific, upon prolonged illumination, the thin films decompose into CsI, PbI₂, and PbBr₂ which can passivate defects and grain boundaries to suppress the non-radiative recombination². Mobile interstitial iodine (I⁰) is attracted by charge carriers accumulated at low energy regions (I-rich domains), whereas the (Br_x⁻) and (I⁰/I⁻) interdiffuse to reduce lattice strain. In this regard, we deduce that the band gap difference between I-rich and Br-rich areas determines the threshold size or the intensity that causes phase segregation. In addition, the lattice strain determines the preferential direction for inter-diffusion of both charge carriers and the iodine mobility, which are responsible for final halide distribution.

The activation energy (E _a) measured in this work		
	CsPbBrI ₂ nanocrystals	CsPbBrI ₂ thin films
Pristine Without COC	20.6 meV	20.8 meV ⁴
Encapsulated With COC	39.3 meV	29 meV ⁴
The activation energy (E _a) of various lead Halide Material		
	Process	The activation energy(E _a)
CsPb(I _{0.5} Br _{0.5}) ₃ Colloidal NCs	Photo-decomposition	62 kJ/mol ⁵
CsPb(Cl _(1-x) Br _x) ₃ Colloidal NCs	Halide Exchange	63 kJ/mol ⁶
PbI ₂ thin film	Photo-decomposition	16 kJ/mol ⁷

Table 1. The activation energy of pristine CsPbI₂Br and encapsulated CsPbI₂Br nanocrystals and films compared to the previous activation energy for various mixed halide compositions.

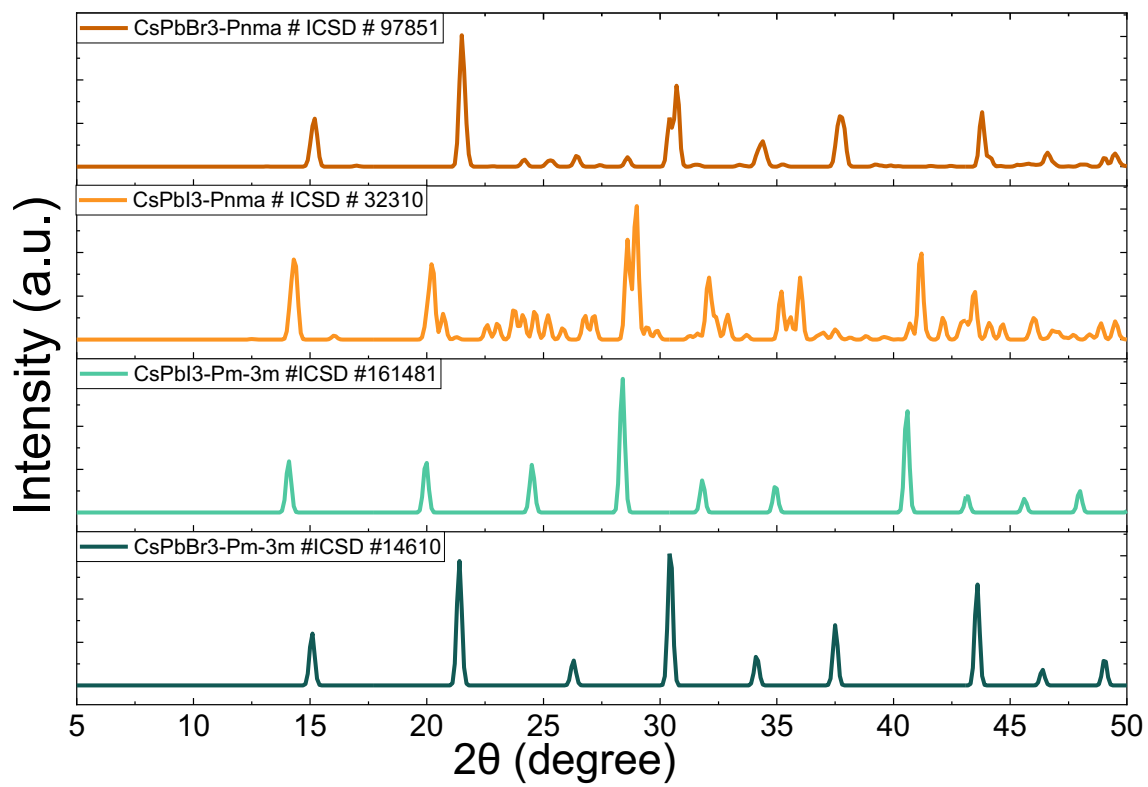


Figure S2. The reference patterns of the orthorhombic, cubic, and tetragonal phases of CsPbBr₃ and CsPbI₃ obtained in the Inorganic Crystal Structure Database (ICSD).

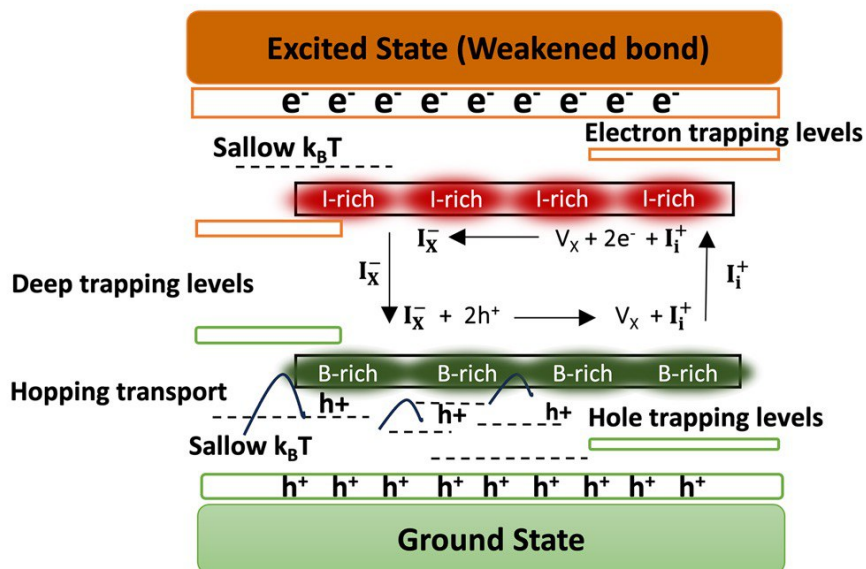


Figure S3. Schematic illustrating the photoinduced halide oxidation mechanism for mixed halide perovskites in the form of CsPbI₂Br nanocrystals and thin films. The photogenerated holes ($2 h^+$) oxidize the lattice iodide ions (I_x^-), leading to the formation of iodine (I_2) and / or triiodide (I_3^-), either in the bulk (I^*) or at surfaces (I^0).³ If it forms in bulk, the (I_2) migrate faster and are then expelled from the lattice, where uncoordinated Pb²⁺ and Cs⁺ ions accumulate at the nanocrystal surface. Meanwhile, the lattice bromine ions (Br_x^-) drift or diffuse into the Br-rich region and reconstruct the CsPbBr₃ instead of photo-decomposition due to a higher oxidation potential than for the lattice iodide (I_x^-).

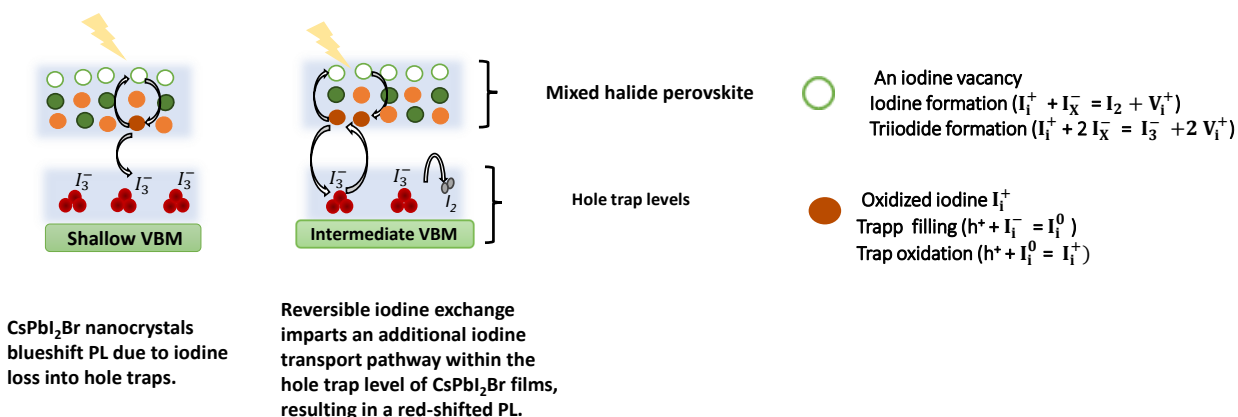


Figure S4. Schematic illustrating the photoinduced halide oxidation mechanism of mixed halide perovskites in the form of CsPbI₂Br nanocrystals and CsPbI₂Br thin films.

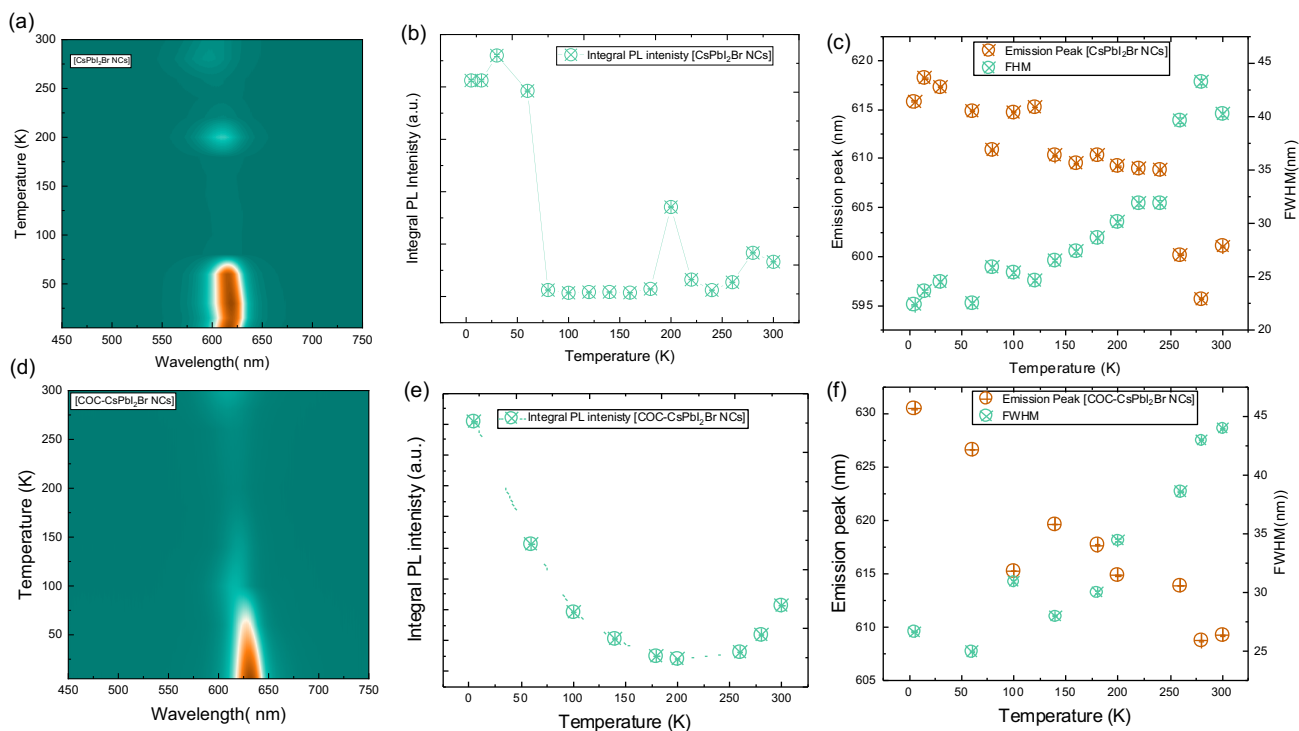


Figure S5. Temperature dependent photoluminescence of CsPbI₂Br nanocrystals and their COC-encapsulated counterparts (a-d) The PL spectra of a 2D -colour plot of the CsPbI₂Br NCs and encapsulated counterparts at temperatures ranging from 5 to 297 K. (b-e) The integrated PL intensity as a function of temperature for CsPbI₂Br nanocrystals and COC-encapsulated CsPbI₂Br (d-e)The emission peak and FWHM as a function of temperature for nanocrystals and COC-encapsulated CsPbI₂Br, respectively.

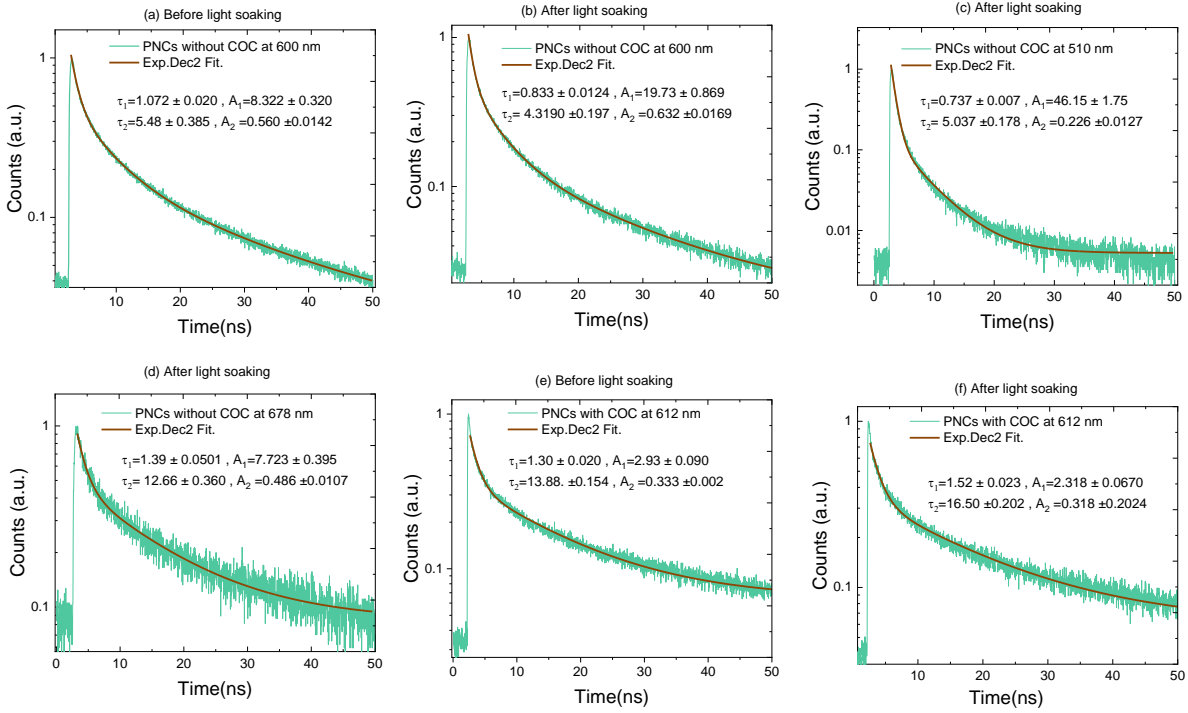


Figure S6. Time decay parameters of CsPbI₂Br nanocrystals and their COC-encapsulated counterparts before and after 50 minutes of a blue light illumination at a wavelength of 450 nm at a laser repetition rate of 7.8 MHz for PNC with COC and 16 MHz for PNCs without COC, respectively. The fitted TRPL decay parameters were extracted using the equation:

$$f(t) = A_1 \exp(-t/\tau_1) + A_2 \exp(-t/\tau_2) + y_0,$$

Where τ_1 refers to short-lived PL emission, and τ_2 represent the long-lived lifetime

References

1. Akriti *et al.* Layer-by-layer anionic diffusion in two-dimensional halide perovskite vertical heterostructures. *Nat. Nanotechnol.* **16**, 584–591 (2021).
2. Chen, Q. *et al.* Controllable self-induced passivation of hybrid lead iodide perovskites toward high performance solar cells. *Nano letters* **14**, 4158–4163 (2014).
3. Kerner, R. A., Xu, Z., Larson, B. W. & Rand, B. P. The role of halide oxidation in perovskite halide phase separation. *Joule* **5**, 2273–2295 (2021).
4. Alanazi, M. *et al.* Stability of mixed lead halide perovskite films encapsulated in cyclic olefin copolymer at room and cryogenic temperatures. *The J. Phys. Chem. Lett.* **14**, 11333–11341 (2023).
5. Brennan, M. C. *et al.* Photolysis of mixed halide perovskite nanocrystals. *ACS Energy Lett.* **8**, 2150–2158 (2023).
6. Scharf, E. *et al.* Ligands mediate anion exchange between colloidal lead-halide perovskite nanocrystals. *Nano Lett.* **22**, 4340–4346 (2022).
7. Dawood, R., Forty, A. & Tubbs, M. The photodecomposition of lead iodide. *Proc. Royal Soc. London. Ser. A. Math. Phys. Sci.* **284**, 272–288 (1965).

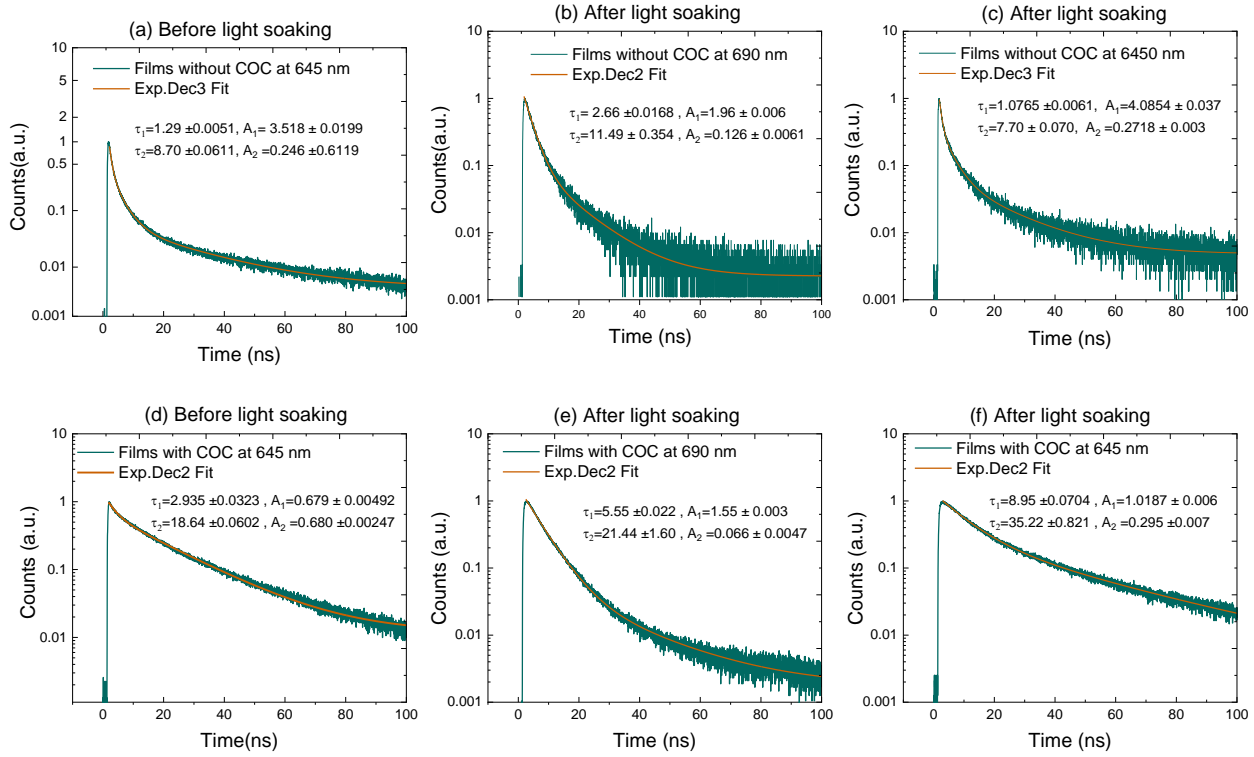


Figure S7. Time decay parameters of CsPbI₂Br thin films and their COC-encapsulated counterparts before and after 50 minutes of a blue light of illumination at a wavelength of 450 nm and a 8.3 MHz laser repetition rate. The fitted TRPL decay parameters were extracted using the equation:

$$f(t) = A_1 \exp(-t/\tau_1) + A_2 \exp(-t/\tau_2) + y_0,$$

Where τ_1 refers to short-lived PL emission, and τ_2 represent the long-lived lifetime